STREGA: STRucture and Evolution of the GAlaxy with the VST

Marcella Marconi[1]
Ilaria Musella[1]
Marcella Di Criscienzo[1,2]
Michele Cignoni[3]
Massimo Dall'Ora[1]
Giuseppe Bono[4]
Vincenzo Ripepi[1]
Enzo Brocato[2]
Gabriella Raimondo[5]
Aniello Grado[1]
Luca Limatola[1]
Giuseppina Coppola[1]
Maria Ida Moretti[1,6]
Peter B. Stetson[7]
Annalisa Calamida[2,3]
Michele Cantiello[5]
Massimo Capaccioli[8]
Enrico Cappellaro[9]
Maria-Rosa L. Cioni[10,11]
Scilla Degl'Innocenti[12]
Domitilla De Martino[1]
Alessandra Di Cecco[2,13]
Ivan Ferraro[2]
Giacinto Iannicola[2]
Pier Giorgio Prada Moroni[12]
Roberto Silvotti[14]
Roberto Buonanno[4,5]
Fedor Getman[1]
Nicola R. Napolitano[1]
Luigi Pulone[2]
Pietro Schipani[1]

[1] INAF-Osservatorio Astronomico di Capodimonte, Naples, Italy
[2] INAF-Osservatorio Astronomico di Roma, Italy
[3] Space Telescope Science Institute, Baltimore, USA
[4] Dipartimento di Fisica, Università degli Studi di Roma-Tor Vergata, Italy
[5] INAF-Osservatorio Astronomico di Teramo, Italy
[6] INAF-Osservatorio Astronomico di Bologna, Italy
[7] NRC-Herzberg, Dominion Astrophysical Observatory, Victoria, Canada
[8] Università "Federico II", Naples, Italy
[9] INAF-Osservatorio Astronomico di Padova, Italy
[10] University of Hertfordshire, Hatfield, UK
[11] Leibnitz-Institut für Astrophysik Potsdam, Germany
[12] Università "E. Fermi", Pisa, Italy
[13] Agenzia Spaziale Italiana Science Data Center (ASDC), Frascati, Italy
[14] INAF-Osservatorio Astrofisico di Torino, Pino Torinese, Italy

STREGA (STRucture and Evolution of the Galaxy) is an ongoing VLT Survey Telescope Guaranteed Time survey, covering an area of about 150 square degrees, aimed at investigating the mechanisms of formation and evolution of the Galactic Halo. The project is organised into two parts: a core programme to search for the signatures of interaction between selected stellar systems and the Galactic Halo and a complementary part focussed on the southern portion of the Fornax Stream. The basis is the use of variable stars (RR Lyrae and long period variables) and main sequence turn-off stars as tracers of stellar overdensities. Observations in *g,r,i* bands, with additional filters, *u*, Strömgren *v* and Hα for selected fields, will allow investigation of the properties of Halo white dwarfs and interacting binaries. We present an overview of the survey and some first results, in particular for the region centred on Omega Centauri.

Scientific context

The study of the Milky Way (MW) and its satellite galaxies is crucial for our understanding of the formation and evolution of galaxies through their interaction with the environment. Several authors (Marconi et al. [2014] and references therein) have shown that the outer regions of the Galactic Halo appear quite clumpy, with a number of observed stellar overdensities, supporting theories based on the hierarchical formation of structures in a cold dark matter cosmological scenario. The most spectacular example of these phenomena is the observed merging of the Sagittarius dwarf spheroidal galaxy with the MW Halo and its associated stream (see e.g., Deg & Widrow [2013] and references therein).

In the Galactic Halo, several other streams have been hypothesised since the pioneering suggestion by Lynden-Bell (1976) that the dwarf spheroidal galaxies (dSphs) orbiting around the MW and a number of Galactic globular clusters (GGCs) are distributed along planar alignments. These are usually interpreted as orbital planes resulting from the disruption of galaxies through the interaction with the Galactic Halo. The location of these systems seems to define a vast polar structure in the MW (see e.g., Pawlowski & Kroupa, 2013). Evidence of a similar plane has recently been claimed for M31 by Conn et al. (2013) and Ibata et al. (2013). The Fornax Stream (Majewski, 1994) is an example of these alignments and includes both dSphs (Fornax, Leo I, Leo II, Sculptor and possibly Sextans and Phoenix) and GGCs (Pal 3, Pal 4 and Pal 12). Extra-tidal stellar populations have been detected around several stellar systems, including both GGCs and dSphs. They define either elongated tidal tails or spheroidal shells formed by material tidally stripped in the interaction of these small systems with the MW (see Marconi et al. [2014] for details).

In this scenario, the VLT Survey Telescope (VST) STREGA survey aims at investigating the formation mechanisms for the Galactic Halo, by tracing tidal tails and haloes around stellar clusters and galaxies and mapping the southern portion of the Fornax Stream.

The STREGA survey

The STREGA survey uses part of the VST Guaranteed Time Observation (GTO) allocated by ESO to the Italian Istituto Nazionale di Astrofisica (INAF) in return for the building of the telescope.

The core programme of STREGA (P.I.: M. Marconi/I. Musella; see also Marconi et al., 2014) is the search for stellar overdensities (tidal tails and/or haloes) through detection of variable and main sequence stars around selected dSphs and GGCs up to 2–3 tidal radii. The investigated systems include: Fornax and Sculptor (38 fields), Sextans (13 fields), Phoenix (3 fields), ω Cen and NGC 6752 (37 and 36 fields, respectively), Pal 3 (3 fields) and Pal 12 (2 fields). The location of the selected targets for the STREGA core programme is shown in Figure 1 (by blue and magenta symbols for dSphs and GGCs, respectively). Variable stars, such as RR Lyrae, are easily detectable thanks to their intrinsic luminosity and characteristic light curves, whereas main sequence turn-off (MSTO) stars are about 3.5 mag fainter than RR Lyrae stars but at least 100 times more abundant. The second part of the survey complements the core programme with additional fields

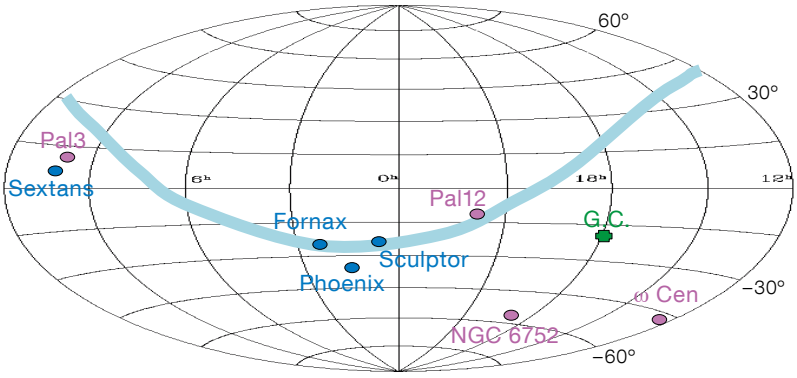

Figure 1. The dSphs (blue symbols) and GGCs (magenta symbols) observed by the STREGA survey. The cyan line represents the orbit of Fornax in equatorial coordinates. The Galactic Centre is marked with a green symbol.

(when needed) and maps the southern portion of the Fornax Stream along strips distributed transverse to the Fornax orbit.

Finally, the STREGA survey has the additional objective of sampling, at various Galactic latitudes, single white dwarfs and interacting binaries in the fields (see Marconi et al. [2014] for further details).

STREGA observing strategy

Owing to its wide field of view and high spatial resolution, OmegaCAM on the VST is the ideal instrument with which to investigate extra-tidal stellar populations or extended haloes around dSphs and GGCs. In our survey, the observations are performed in the SDSS filters *g*, *r* and *i*. We adopt three bands to characterise variable and MSTO stars and provide colour–magnitude and colour–colour diagrams for the investigated stellar populations. In particular, the light curves of the variable stars are accurately sampled by means of time-series observations (about 20 phase points in *g*-band and 10 in *r*- and *i*-bands). The MSTO magnitude is reached by co-addition of single epoch observations or through direct deeper exposures for close systems such as ω Cen, NGC 6752 and Pal 12. Indeed, the exposure times of a few seconds needed to reach the RR Lyrae magnitude level in these clusters are dramatically shorter than telescope overheads. In these cases variability could be investigated with follow-up observations, at other telescopes, on selected fields.

Observations and data reduction

The 2.6-metre VST optical survey telescope (Capaccioli & Schipani, 2011), built by INAF–Osservatorio Astronomico di Capodimonte, Naples, Italy, is equipped with OmegaCAM (Kuijken, 2011), a wide field (1 by 1 degree) camera provided by a consortium of European institutes. It is a 32-CCD, 16k by 16k detector mosaic with a pixel scale of 0.214 arcseconds.

Observations for the VST INAF GTO started at the end of 2011. STREGA proposals have been approved for Periods 88–94. Due to technical and scheduling problems, only a minor part (about 25 %) of the STREGA core programme has been observed so far. In particular, observations have been completed for the fields around ω Cen (observed in ESO Period 88 and in the compensating visitor time in March 2013), NGC 6752 (Periods 89, 93) and Pal 12 (Periods 91, 93).

The data reduction is performed by means of the newly developed VST–Tube imaging pipeline (Grado et al., 2012), specifically conceived for the data from the VST telescope, but adaptable to other single or multi-CCD cameras. The pipeline includes the over-scan, bias and flat-field correction, CCD gain harmonisation and illumination correction. For the individual exposures, relative and absolute astrometric and photometric calibration is applied (see Marconi et al. [2014] for details).

In order to obtain accurate stellar photometry in the crowded stellar clusters, we need to use a package that performs a point spread function (PSF) fitting method (e.g., Stetson, 1987), while for uncrowded fields, we can also adopt aperture photometry. In particular, we use DAOPHOT/ALLSTAR (Stetson, 1987) for the crowded fields, and SExtractor (Bertin & Arnouts, 1996) for the uncrowded ones. The latter package, usually adopted for extragalactic studies, gives accurate results for stellar photometry in uncrowded fields and has the advantage of being fast and fully automated. We have checked the consistency of the two kinds of photometry by comparing the SExtractor measurements with the DAOPHOT/ALLSTAR ones for selected images (Marconi et al., 2014).

Concerning the completed observational runs, the photometry on the four fields including the central part of ω Cen and on the two fields centred on Pal 12, was obtained using the DAOPHOT/ALLSTAR packages. To calibrate the photometry of the four central pointings on ω Cen, observed in non-photometric conditions, we used deep and accurate *UBVRI* photometry by Castellani et al. (2007), transformed to the SDSS *ugriz* photometric system by adopting the transformations by Jordi et al. (2006) computed for Population II stars[1]. Similarly for Pal 12, we checked the photometric calibration using independent and very accurate unpublished *BVI* photometry by Peter Stetson. In the case of NGC 6752, due to the very recent observations of the central region, the calibration procedure is still in progress and so far we have only qualitatively verified the agreement between our colour–magnitude diagrams (CMDs) for the external fields and the central one obtained from unpublished photometry by Stetson (see Marconi et al., 2014 for details). In the following, we show the first results obtained for the fields centred on ω Cen.

The total CMD for the ω Cen sky area

Among the stellar systems that we are currently investigating in the context of the STREGA core programme, a particularly interesting target is ω Cen. This globular cluster is considered to be a tidally disrupted galaxy due to: i) the presence of multi-populations with different chemical compositions (and probably

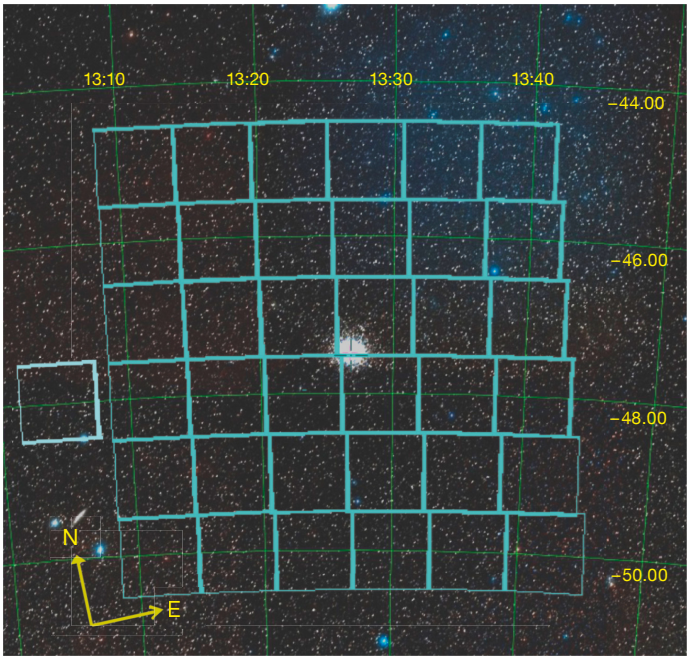

Figure 2. Observed STREGA fields around ω Cen shown in equatorial coordinates.

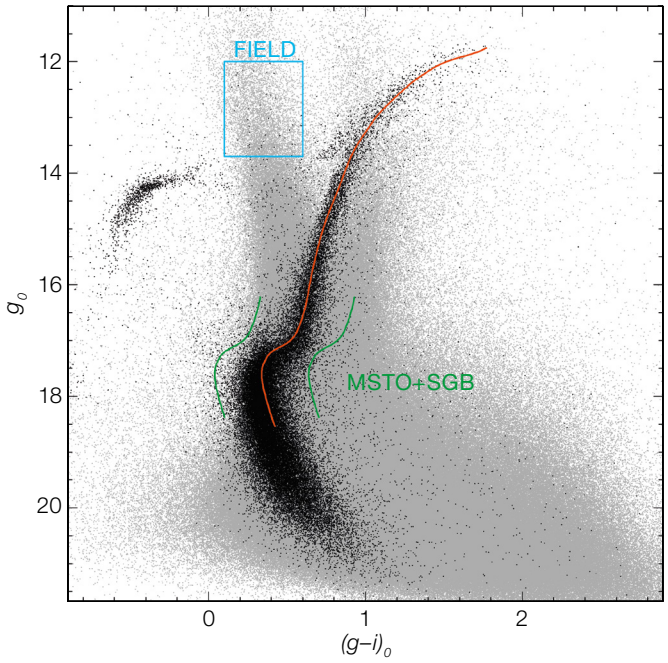

Figure 3. Cumulative CMD (grey dots) compared with the central CMD (black dots) for ω Cen. The red line represents the obtained ridgeline.

different ages); ii) the retrograde orbit combined with an unusually low inclination; iii) the similarity with M54, a globular cluster that is the remnant core of the disrupted Sagittarius galaxy. The presence of tidally stripped stars for ω Cen has been modelled, but only very recently have Majewski et al. (2012) reported empirical evidence for these tidal tails. We have observed, with the VST, the 37 fields shown in Figure 2, centred on ω Cen and reaching about three tidal radii.

Each field is observed in *gri*-bands with a single exposure reaching at least 2 mag below the turn-off. Combining the *g*, *r* and *i* catalogues for all the covered fields, we built the total CMDs *g,g-i* and *g,g-r*. To search for overdensities associated with various evolutionary phases in the CMD, we needed to take into proper account the differential reddening contribution as well as the contamination from the various Galactic components. In order to correct for the reddening in the observed fields, we used the extinction maps of Schlegel et al. (1998), recalibrated by Schlafly & Finkbeiner (2011)[2]. The de-reddened *g,g-i* diagram is shown in Figure 3 (see the following section for details).

In order to model the contribution of the different MW components to the CMD, we used an updated version of the code by Castellani et al. (2002), including three Galactic components, namely the thin and thick Disc and a stellar Halo, with specific spatial structures and star formation laws (see Marconi et al. [2014] for details). Due to the low Galactic latitude, we expect that our CMD is mainly contaminated by thin and thick Disc stars with a smaller fraction of Halo stars. The result of this Galactic simulation for one of the investigated fields is shown in Figure 4 (blue, cyan and grey dots) compared with the synthetic CMD of ω Cen (red symbols) obtained with the SPOT code (Teramo Stellar POpulation Tools; Raimondo et al., 2005). We note that, according to these simulations, it is possible to distinguish the bluest MSTO from the Galactic Disc population.

Extra-tidal stars of ω Cen

We performed star counts on the area observed around ω Cen in order to detect extra-tidal stars. First, we evaluated the photometric completeness to find, in each band, the range of magnitudes where star counts are significant (see Marconi et al. [2014] for details). We considered the central CMD (black dots in Figure 3) obtained on the one square degree field centred on ω Cen to identify the expected location of the various evolutionary phases, namely the horizontal branch, the MSTO and the red giant branch. The red line in Figure 3 represents the empirical ridgeline obtained from the observed central CMD. All the sources lying within ± 0.3 mag (between the green lines), consistent with the dispersion of the MSTO region and with possible residual differential reddening and/or photometric errors and in the magnitude range $16.2 < g_0 < 18.5$ mag, are assumed to belong to the MSTO and sub-giant branch phase (MSTO+SGB). We also identified a region (called FIELD, see blue rectangle in Figure 3) without cluster contamination, corresponding to the ranges $12.0 < g_0 < 13.7$ mag and $0.1 < (g\text{-}i)_0 < 0.6$ mag.

In the left-hand panels of Figure 5 we show the radial profiles of the normalised star densities in the MSTO+SGB region, compared to those in the FIELD region where we expect a negligible contribution of cluster stars. The error bars are the result of the individual count Poisson error.

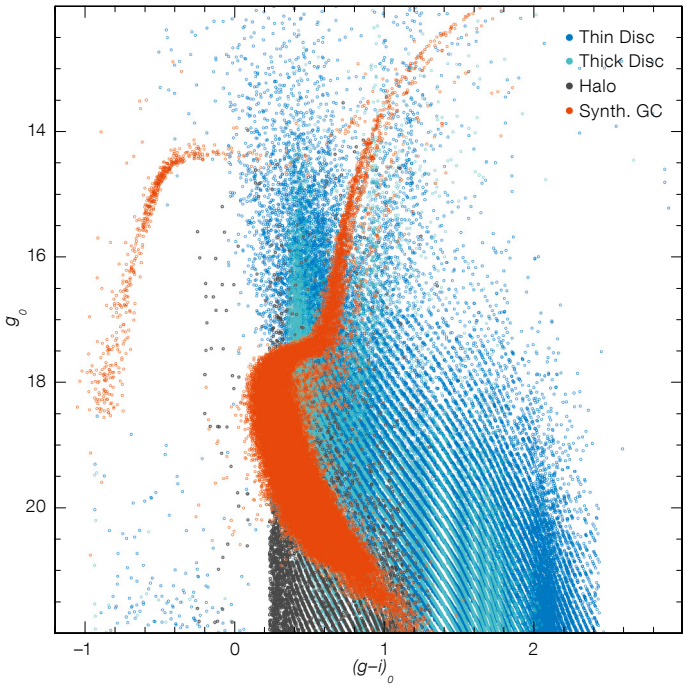

Figure 4. Galactic simulations (blue, cyan and grey dots) compared with the synthetic CMD of ω Cen (red dots).

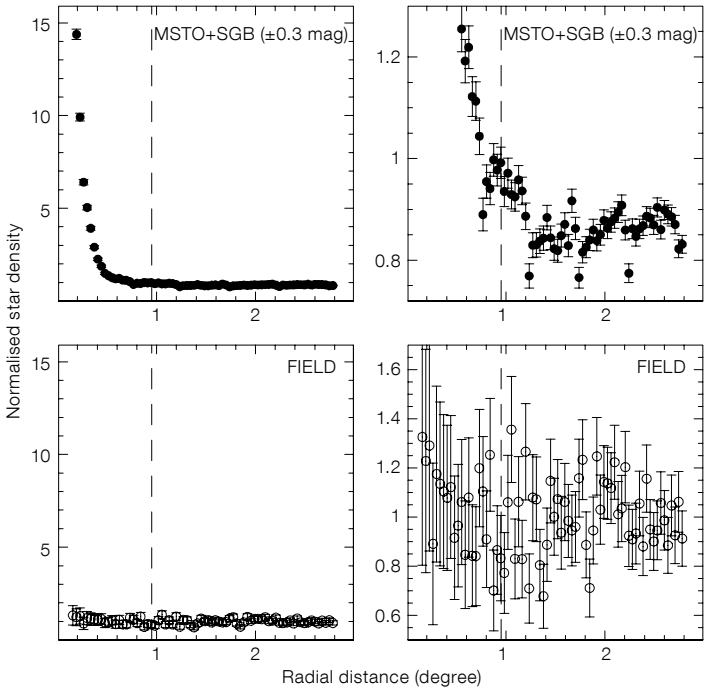

Figure 5. Left-hand panels: Radial profiles of the normalised star densities for ω Cen for objects in the MSTO+SGB and FIELD regions of the CMD (upper and lower respectively). Right hand panels: Zoom-in of the left panels around the nominal tidal radius.

We covered the region from the centre to 2.8 degrees (about three nominal tidal radii) with 75 equally spaced annuli. The star density in the i^{th} annulus is normalised to the corresponding total count in the circle with the radius of 2.8 degrees. The nominal tidal radius (0.95 degrees, corresponding to the vertical dashed line in Figure 5; see Harris, 1996; Da Costa & Coleman, 2008) is intermediate between the two values provided by McLaughlin & van der Marel (2005), adopting a King model (0.80 degrees; King, 1966) and a Wilson model (1.2 degrees; Wilson 1975),

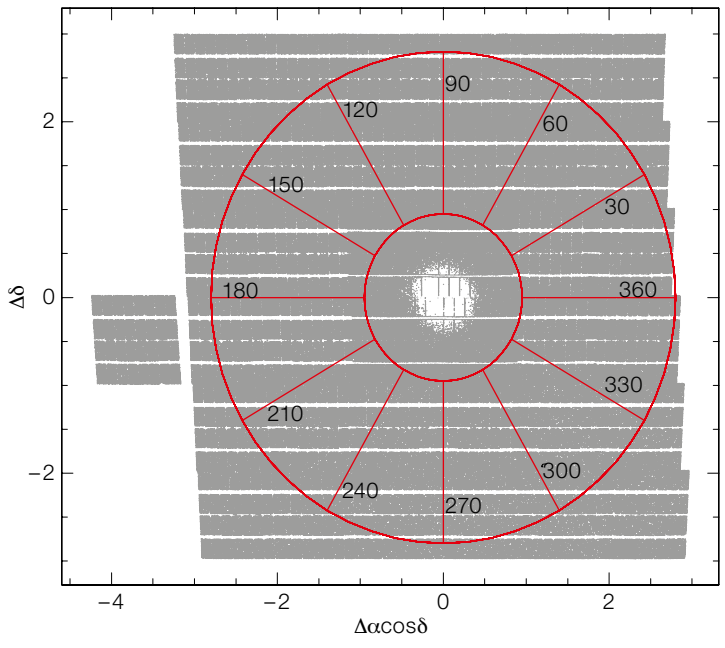

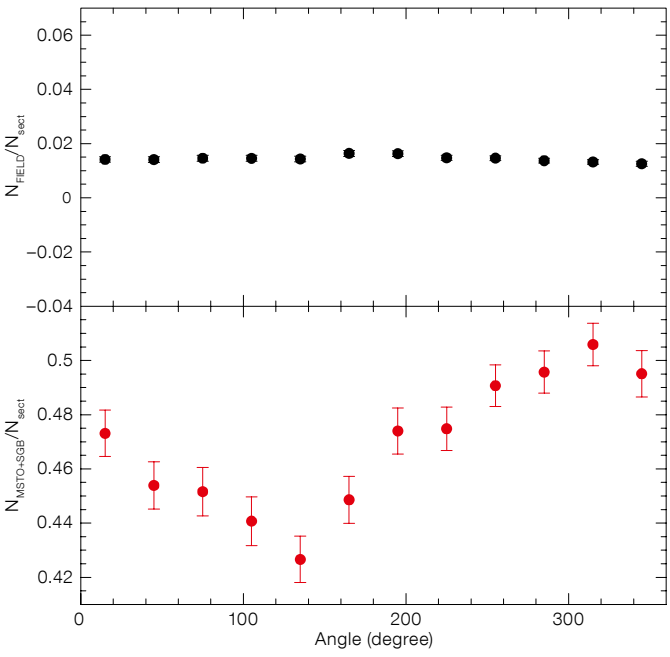

Figure 6. Left panel: Circular sectors used for the angular star counts around ω Cen. Right panel: Normalised star counts for MSTO+SGB (red dots) and FIELD stars (black dots) in the angular sectors shown in the left panel.

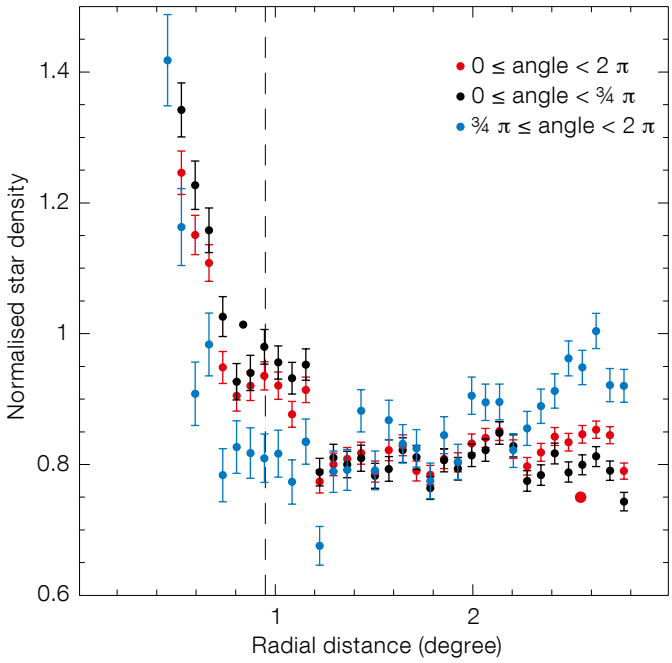

Figure 7. Radial profile of the normalised star densities for the ω Cen MSTO+SGB stars in the different labelled angular regions.

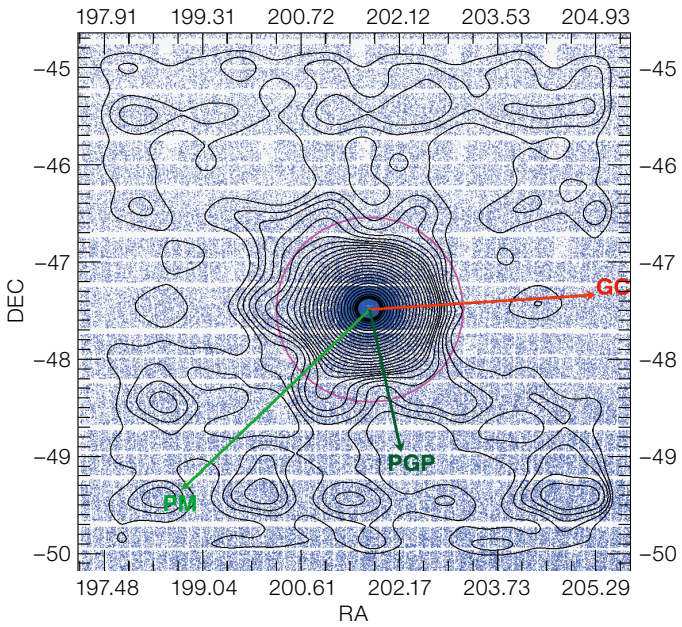

Figure 8. Contour level of the stars around ω Cen projected on the sky. Orientation is the same as in Figure 2. The long light green arrow shows the direction of proper motion (PM); see text for details.

respectively. We recall that the evaluation of the tidal radius is not only model-dependent (McLaughlin & van der Marel, 2005) but also difficult to obtain on account of the possible contribution of tidal tails or other kinds of extra-tidal stellar population (see e.g., Di Cecco et al. [2013] and references therein).

The right-hand panels of Figure 5 show a zoom of these plots to highlight the behaviour around the tidal radius. While, as expected, the FIELD stars do not show any specific trend, the MSTO+SGB stars follow the typical globular cluster profile (see e.g., King, 1966; Wilson, 1975). Inspection of this plot suggests that the nominal tidal radius is slightly underestimated. According to the observed MSTO+SGB star counts, the value based on the Wilson model (1.2 degrees; McLaughlin & van der Marel, 2005) seems to be more in agreement with the data, with an additional non-negligible density increase around and beyond two nominal tidal radii. The latter evidence could be the signature of the presence of tidal tails.

To verify this hypothesis we decided to consider the MSTO+SGB star counts also as a function of the direction, by dividing the total explored area into twelve 30-degree circular sectors (see left-hand panel of Figure 6), with a radial distance ranging from one to three tidal radii. The MSTO+SGB star counts in the sectors are normalised to the total number of stars in the same area, in order to reduce spurious effects due to the variation of the disc contribution with Galactic latitude.

The MSTO+SGB star counts as a function of angle are shown in the lower right-hand panel of Figure 6, where a clear peak is observed around 300 degrees (the south-east direction). This corresponds to the predicted orientation of the cluster ellipticity (see e.g., Table 5 in Anderson & van der Marel, 2010). It is also significant that FIELD star counts (upper right-hand panel) do not follow the same trend.

In Figure 7, the MSTO+SGB star count radial profile in the direction corresponding to the overdensity (blue filled circles) is compared with the total one (red filled circles) and with the one in the complement to 2π (black filled circles). This comparison shows how the radial profile varies with the angle: the star overdensity detected beyond the tidal radius is more evident to the southeast. Moreover, even excluding this overdensity direction and looking at the radial profile in the opposite direction (black filled circles), we find an excess of stars at about 1 degree from the centre, corresponding to an effective tidal radius of about 1.2 degrees.

Similar behaviour can also be noted in the contour level map, again for the MSTO+SGB candidate cluster stars, shown in Figure 8 (see Marconi et al. [2014] for details). The excess of stars beyond the nominal tidal radius (0.95 degrees, magenta circles) is evident in the second, third and fourth quadrants (usual clockwise definition) where it extends up to about 2 degrees, confirming the evidence of extra- tidal stars inferred from Figure 5.

Inspection of Figure 8 also suggests that the asymmetry of the contour levels increases when moving from the innermost to the outermost cluster regions. This result agrees with the evaluation of ω Cen eccentricity in the literature (e.g., Bianchini et al., 2013). Finally we note that the detected overdensity orientation in Figure 8 appears to be orthogonal

to ω Cen's proper motion direction (PM, green arrow) and intermediate between the direction of the Galactic Centre (GC, red arrow) and the projection on the sky of the direction perpendicular to the Galactic Plane (PGP, dark green arrow). The position angle of the major axis indicated by these star counts, measured east from north, is about 140 degrees and agrees quite well with the one based on Hubble Space Telescope Advanced Camera for Surveys photometry of the innermost cluster regions (Anderson & van der Marel, 2010). Even though to understand the nature of the detected extra-tidal stars, the information on their proper motion and radial velocity is needed, the presence of an asymmetric, elongated extra-tidal structure is evident and consistent with current measurements and predictions in the literature for the cluster ellipticity profile and orientation.

The preliminary results shown here clearly demonstrate the wealth of information that can be extracted from the VST observations. On this basis, when the STREGA survey is complete we will be able to significantly improve our knowledge of Galactic structure and evolution, providing useful constraints complementary to the geometric information that will be inferred with the Gaia satellite.

References

Anderson, J. & van der Marel, R. P. 2010, ApJ, 710, 1032
Bertin, E. & Arnouts, S. 1996, A&AS, 117, 393
Bianchini, P. et al. 2013, ApJ, 772, 67
Capaccioli, M. & Schipani, P. 2011, The Messenger, 146, 2
Castellani, V. et al. 2002, MNRAS, 334, 69
Castellani, V. et al. 2007, ApJ, 663, 1021
Conn, A. R. et al. 2013, ApJ, 766, 120
Da Costa, G. S. & Coleman, M. G. 2008, AJ, 136, 506
Deg, N. & Widrow, L. 2013, MNRAS, 428, 912
Di Cecco, A. et al. 2013, AJ, 145, 103
Grado, A. et al. 2012, Mem. Soc. Astron. Ital. Suppl., 19, 362
Harris, W. E. 1996, AJ, 112, 148
Ibata, R. A. et al. 2013, Nature, 493, 62
King, I. R. 1966, AJ, 71, 64
Kuijken, K. 2011, The Messenger, 146, 8
Lynden-Bell, D. 1976, MNRAS, 174, 695
Majewski, S. R. et al. 2012, ApJ, 747, L37
Marconi, M. et al. 2014, MNRAS, in press, arXiv:1406.4375
McLaughlin, D. E. & van der Marel, R. P. 2005, ApJS, 161, 304
Pawlowski, M. S. & Kroupa, P. 2013, MNRAS, 435, 2116
Raimondo, G. et al. 2005, AJ, 130, 2625
Schlegel, D. J., Finkbeiner, D. P. & Davis, M. 1998, ApJ, 500, 525
Stetson, P. 1987, PASP, 99, 191
Wilson, C. P. 1975, AJ, 80, 175

Links

[1] *UBVRI* to SDSS *griz* transformations: http://classic.sdss.org/dr7/algorithms/sdssUBVRITransform.html#Jordi2006
[2] Recalibrated Schlegel extinction: http://irsa.ipac.caltech.edu/applications/DUST/

ESO/INAF-VST/OmegaCAM. Acknowledgement: A. Grado/INAF-Capodimonte Observatory

Large-field (51 arcminute square) image of the globular cluster ω Cen taken with the VLT Survey Telescope by combining *g*-, *r*- and *i*-band images.